



Discovery and SAR of potent, orally available 2,8-diaryl-quinoxalines as a new class of JAK2 inhibitors

Carole Pissot-Soldermann*, Marc Gerspacher, Pascal Furet, Christoph Gaul, Philipp Holzer, Clive McCarthy, Thomas Radimerski, Catherine H. Regnier, Fabienne Baffert, Peter Druedes, Gisele A. Tavares, Eric Vangrevelinghe, Francesca Blasco, Giorgio Ottaviani, Flavio Ossola, Julien Scesa, Janitha Reetz

Novartis Institutes for Biomedical Research, Novartis Pharma AG, WKL-136.4.96, CH-4002 Basel, Switzerland

ARTICLE INFO

Article history:

Received 18 December 2009

Revised 13 February 2010

Accepted 16 February 2010

Available online 19 February 2010

Keywords:

Janus kinase

JAK1

JAK2

JAK3

Tyk2

Kinase inhibitors

ABSTRACT

We have designed and synthesized a novel series of 2,8-diaryl-quinoxalines as Janus kinase 2 inhibitors. Many of the inhibitors show low nanomolar activity against JAK2 and potently suppress proliferation of SET-2 cells *in vitro*. In addition, compounds from this series have favorable rat pharmacokinetic properties suitable for *in vivo* efficacy evaluation.

© 2010 Elsevier Ltd. All rights reserved.

The Janus kinase (JAK) family comprises of four non-receptor protein tyrosine kinases, JAK1, JAK2, JAK3 and TYK2, which play an important role in cell survival, proliferation and differentiation.¹ The discovery of somatic mutations in JAK2, particularly that of JAK2^{V617F}, in patients with chronic myeloproliferative neoplasms (MPNs) marked an important milestone in our understanding of the pathogenesis of these disorders.^{2,3} The JAK2^{V617F} mutation is present in nearly every patient with polycythemia vera and in almost 50% of patients with essential thrombocythemia or primary myelofibrosis.⁴ Thus, JAK2 represents a promising target for the treatment of MPNs and considerable efforts are ongoing to discover and develop small molecule inhibitors of its kinase activity. Herein, we describe the discovery of 2,8-diaryl-quinoxalines as potent JAK2 inhibitors, and report on their JAK family selectivity, anti-proliferative effects in JAK2^{V617F} bearing SET-2 cells and pharmacokinetic properties in rats.

Screening an internal proprietary kinase compound collection resulted in the identification of a lead compound, which through iterative scaffold morphing exercises^{5,6} and optimization afforded a class of 2,8-diaryl-quinoxalines, represented by the prototype compound (**1**; Fig. 1). Compound **1** is a potent inhibitor of JAK2 (IC₅₀ = 42 nM), with a 30-fold JAK2/JAK3 selectivity in enzymatic assays and an overall favorable kinase selectivity profile. The hypo-

thetical binding mode for this compound was confirmed by the crystal structure of the active JAK2 protein kinase domain in complex with **1** (Fig. 2)⁷ and revealed that the quinoxaline N1 atom is involved in a critical interaction with the hinge part of the kinase through a hydrogen-bond with the backbone amide of Leu932. In addition, this quinoxaline ring makes hydrophobic contacts with side chains of residues Ala880, Met929 and Leu983. Favorable hydrophobic contacts are also observed between the aromatic ring of the trimethoxyphenyl substituent of **1** and the side chain of Leu855 and backbone of Gly935. The methylsulfonamide group participates in multiple hydrogen-bond interactions with water molecules located in the phosphate region of the ATP binding site. The phenyl ring that links the quinoxaline core to the methylsulfonamide moiety, occupies a hydrophobic part of the cavity, surrounded by the side chains Val863, Leu983 and backbone of Gly993.

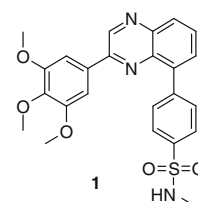


Figure 1. Structure of prototype 2,8-diaryl-quinoxaline (**1**).

* Corresponding author. Tel.: +41 61 696 18 90; fax: +41 61 696 62 46.

E-mail address: carole.pissot@novartis.com (C. Pissot-Soldermann).

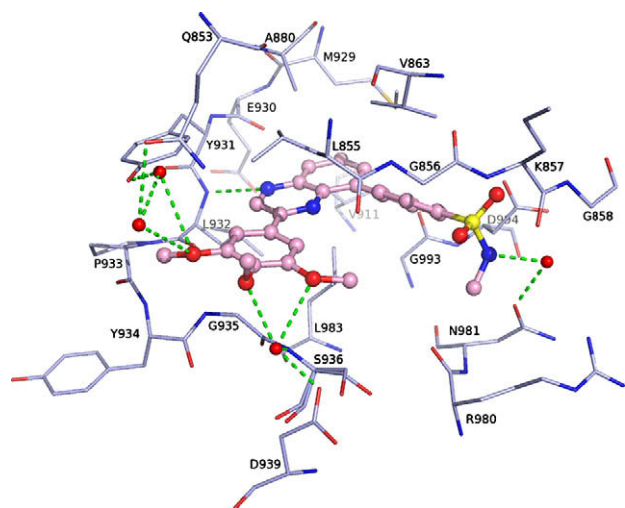
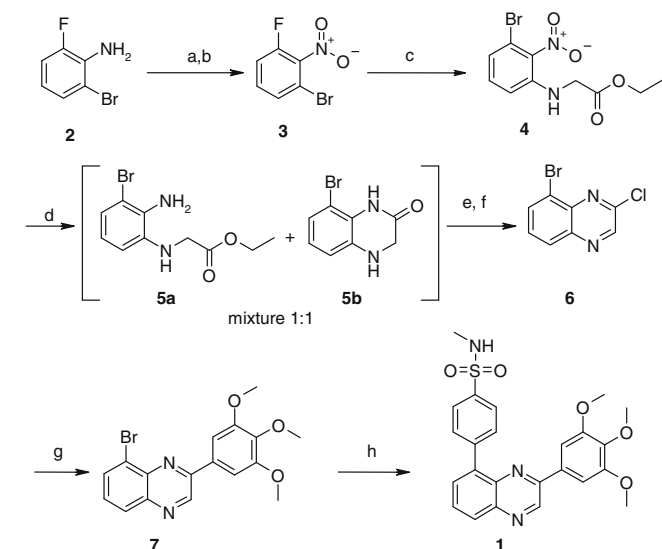


Figure 2. Crystal structure of **1** in complex with the JAK2 kinase domain solved at 2.00 Å resolution. Polar contacts between the inhibitor, solvent and the protein are indicated with dotted lines.

The pharmacokinetic profile of **1** was evaluated in conscious rats. After intravenous bolus administration, **1** shows a rather high total clearance ($87 \text{ mL min}^{-1} \text{ kg}^{-1}$) with a large volume of distribution (6.75 L kg^{-1}) and a moderate terminal half-life (1.69 h) and, after oral administration (3 mg/kg as a suspension in 0.5% carboxymethyl cellulose in bidistilled water) the AUC was $4 \mu\text{g min mL}^{-1}$, corresponding to 34% oral bioavailability.

Based upon the *in vitro/in vivo* profile of **1**, we considered this chemotype as an attractive starting point and embarked on an extensive medicinal chemistry program to optimize the molecule.

The compounds were readily synthesized via the sequence outlined in Scheme 1, starting from 2-bromo-6-fluoro-aniline (**2**). Oxidation of the aniline in two steps yielded the nitro compound (**3**) and fluoride displacement with ethyl glycinate afforded (**4**). Reduction of the nitro group via hydrogenation in the presence of Raney-



Scheme 1. Reagents and conditions: (a) *m*CpBA, CH_2Cl_2 , reflux, 30 min 93%; (b) H_2O_2 30% AcOH, fuming HNO_3 , rt then 90°C , 30 min 66% (crude); (c) ethylglycinate-HCl, DMA, DIEA, 80°C , 18 h, 62%; (d) H_2 , Raney, EtOH, THF 1:1, quant. (crude); (e) *t*-BuOK, THF, MeOH, air, rt, 16 h, 66%; (f) POCl_3 , 55°C , 3 h, 88%; (g) 3,4,5-trimethoxyphenylboronic acid, $\text{Pd}(\text{PPh}_3)_4$, Na_2CO_3 , DMF, 105°C , 68%; (h) *S*-Phos, $\text{Pd}_2(\text{dba})_3$, K_3PO_4 , 1,2-DME, 4-*N*-methyl (aminosulfonylphenyl) boronic acid, 110°C , 15 h, 71%.

Nickel led to a mixture of the corresponding aniline derivative **5a** and the cyclized intermediate **5b**. Treatment of this mixture with *t*-BuOK in the presence of air (oxygen) yielded 8-bromo-1*H*-quinoxaline-2-one which was chlorinated with POCl_3 to provide 8-bromo-2-chloroquinoline (**6**). Intermediate (**6**) was used to introduce structural diversity in the two final steps via consecutive selective palladium-catalyzed Suzuki coupling reactions to introduce two aryl moieties.

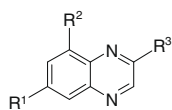
The effects of the 2,8-diaryl-quinoxalines on JAK family members were assessed in biochemical and JAK2-dependent cellular assays (Table 2).^{8,9} The initial SAR studies focused on variation of substituent R^2 . Replacement of the methyl sulfonamide by 4-phenylacetic morpholine amide (**8**) or 4-phenylacetic thiomorpholine dioxide amide (**9**) gave a 3–8 fold gain in JAK2 potency, which also translated into cell growth inhibition (GI_{50}) of 228 nM and 119 nM, respectively, in the SET-2 JAK2^{V617F} proliferation assay. Reducing the planar morpholine amide moiety to the more flexible and slightly basic benzyl morpholine was tolerated (compare **13** with **14** and **15** with **16**). Exploration of the effect of additional small substituents (F or Me) on the phenyl ring in R^2 showed that introduction in the *meta*-position resulted in a fourfold increase in potency (compare entry **13** with **16** and **17**), whereas the same residues in the *ortho*-position yielded a drastic loss of potency (compare entries **18** and **19** with **13**). In comparison to **22**, introduction of a 3,5-difluoro substituent further improved JAK2 inhibitory activity providing compound **23** with a very good inhibition of SET-2 JAK2^{V617F} cell proliferation ($\text{GI}_{50} = 135 \text{ nM}$). This SAR is fully supported by the crystal structure of JAK2 in complex with **1**. This structure suggests that *meta*-substituents can provide additional favorable hydrophobic contacts with residues Val863 and Gly856 of the P-loop on the one hand and the carbon atoms of the side chain of Asp994 on the other hand. In contrast, *ortho*-substituents, by increasing the twist between the quinoxaline core and the phenyl ring R^2 , lead to a steric clash of the substituent with either Val863 or Leu983. As already mentioned, the phenyl ring in R^2 lay in proximity to the backbone of Gly993, which corresponds to Ala966 in JAK3. This difference, coupled with the observation that in a structure of JAK3 recently disclosed¹⁰, Ala966 adopts a ψ backbone conformation of opposite direction compared to that of Gly993 in JAK2 provides a rationale to explain the selectivity for JAK2 against JAK3 obtained with our analogs. The R^2 phenyl ring and its substituents appear to be better accommodated by the less sterically demanding Gly993 residue of JAK2. Introduction of small R^1 groups (F or Me) resulted in significant loss of potency (entry **11** and **12**). As expected from the structure, this R^1 position is too close to the carbonyl group of Glu930 to tolerate any substituent.

Exploration of the R^3 substituent was pursued to optimize the physicochemical properties of the compounds as well as to improve JAK2 affinity (compare **10** with **20** and **15** with **21**). The R^3 substituent is located in the hydrophobic channel formed by residues Gly935 and Leu855 at the entrance of the cavity. Compounds **20** to **23**, in which the trimethoxyphenyl moiety is replaced by carboxamide-substituted phenyl residues, show potent cellular

Table 1
Comparison of measured molecular properties of compounds^{11,12}

Compounds	Log $1/S_0$ (M)	Log <i>P</i>	ΔSL	MP	pK_a
20	4.80	2.80	2.00	204.03	3.9/6.5
24	4.60	4.00	0.60	168.41	4.5/7.2
25	5.06	3.80	1.26	227.28	3.6/6.9
26	3.98	3.20	0.78	137.30	5.5/9.1

S_0 , intrinsic aqueous solubility, Log *P* logarithm of the partition coefficient *P*, based on experimental Log *P*, $\Delta\text{SL} = \text{Log } 1/S_0 - \text{Log } P$, MP: melting point, pK_a : (minus) logarithm of the ionization constant K_a , measured by potentiometry.

Table 2Effects of compounds **1**, and **8–26** on enzymatic activity of JAK family kinases and on cell proliferation in SET-2 JAK2^{V617F} cells^{8,9}

Compds	R ¹	R ²	R ³	JAK1 IC ₅₀ (nM)	JAK2 IC ₅₀ (nM)	JAK3 IC ₅₀ (nM)	TYK2 IC ₅₀ (nM)	Inhibition of SET-2 JAK2 ^{V617F} proliferation GI ₅₀ (nM)
1	H			130	42	1300	640	n.d.
8	H			91	13	1300	640	228
9	H			35	5.1	280	340	119
10	H			98	14	360	520	n.d.
11	Me			>10,000	4200	>10,000	>10,000	n.d.
12	F			940	101	>10,000	>10,000	n.d.
13	H			390	72	2500	2900	n.d.
14	H			1500	120	>10,000	>10,000	n.d.
15	H			1850	195	8300	7130	n.d.
16	H			460	20	1500	1400	n.d.
17	H			250	20	4900	2200	n.d.
18	H			1200	685	2700	4200	n.d.
19	H			4700	501	9900	9300	n.d.

(continued on next page)

Table 2 (continued)

Comps	R ¹	R ²	R ³	JAK1 IC ₅₀ (nM)	JAK2 IC ₅₀ (nM)	JAK3 IC ₅₀ (nM)	TYK2 IC ₅₀ (nM)	Inhibition of SET-2 JAK2 ^{V617F} proliferation GI ₅₀ (nM)
20	H			89	7.1	232	330	96
21	H			362	13	408	439	n.d.
22	H			190	12.5	630	520	226
23	H			60	3.1	130	120	135
24	H			28	4.3	166	94	152
25	H			82	6.8	230	86	98
26	H			303	7.3	610	384	88

activity, but have similar poor water solubility as the prototype compound **1**. In order to understand the main factor causing the low aqueous solubility, we examined the molecular properties of the compounds (Table 1),¹¹ and it appears that the high crystal lattice energy of compound **20** (mp = 204 °C), limits its solubility. Introducing solubilizing groups, as in compounds **24** and **25**, maintained good potency and selectivity, but did not afford good aqueous solubility (0.004 mg mL⁻¹ at pH 6.8 for both compounds). However, the solubility of **24** is limited by lipophilicity, whereas a high crystal lattice energy limits the solubility of **25**.¹¹ Introduction of a piperidinyl-pyrazole residue afforded **26** which has very good solubility (>1.5 mg/mL at pH 6.8) and maintains very good cellular potency (GI₅₀ = 51 nM), together with attractive JAK2 kinase selectivity (at least 40-fold over JAK1, 80-fold over JAK3 and 50-fold over TYK2) and good overall kinase selectivity (the only other kinase in a panel of 36 kinases inhibited with IC₅₀ values <100 nM was ABL (IC₅₀ = 80 nM)).

As the most promising compounds, **24**, **25** and **26** were selected for pharmacokinetic studies in rats (Table 3),¹³ and showed low to moderate clearance, a high volume of distribution and a long elimination half-life after administration of 1 mg/kg iv. After oral administration of 3 mg/kg, all three compounds **24–26** exhibited

Table 3
Effects of compounds **24–26** on pharmacokinetic parameters following administration to rats^{a,13}

Parameters	Compounds		
	24	25	26
Thermodynamic solubility (g/L) pH 6.8	0.004	0.004	>1.5
CL (iv) (mL/min/kg)	19	39	23
V _{ss} (L/kg)	18.9	13.2	33
t _{1/2} (h)	13.4	4.8	18.4
AUC (iv) nmol h L ⁻¹ dn ^b	1653	760	1472
AUC (po) nmol h L ⁻¹ dn ^b	1981	912	449
T _{max} (h)	5.8	8	7.0
C _{max} (nM) dn ^b	74	47	16
Oral %F	~100	~100	31

^a Mean of four animals.

^b Dose-normalized, that is, calculated to a dose of 1 mg/kg.

a low C_{max}, a late T_{max} and an absolute oral bioavailability ranging from 31% to 100%.

In summary, we have discovered a series of selective and potent JAK2 inhibitors. Optimization of the 2,8-diaryl-quinoxalines led to analogs such as **26**, an orally bioavailable small molecule ATP-com-

petitive inhibitor of V617F mutant and wild type JAK2 protein having reduced clearance, improved half-life and superior oral bio-availability compared to the prototype compound **1**.

References and notes

1. Rane, S. G.; Reddy, E. P. *Oncogene* **2000**, *19*, 5662.
2. Levine, R. L.; Pardanani, A.; Tefferi, A.; Gilliland, D. G. *Nat. Rev. Cancer* **2007**, *7*, 673.
3. Tefferi, A.; Vardiman, J. W. *Leukemia* **2008**, *22*, 14.
4. Tefferi, A.; Gilliland, D. G. *Cell Cycle* **2005**, *4*, 1053.
5. Furet, P.; Gerspacher, M.; Pissot-Soldermann, C. *Bioorg. Med. Chem. Lett.* **2010**, *20*, 1858.
6. Gerspacher, M.; Furet, P.; Pissot-Soldermann, C.; Gaul, C.; Holzer, P.; Vangrevelinghe, E.; Lang, M.; Erdmann, D.; Radimerski, T.; Regnier, C. H.; Chene, P.; De Pover, A.; Hofmann, F.; Baffert, F.; Buhl, T.; Aichholz, R.; Blasco, F.; Endres, R.; Trappe, J.; Druce, P. *Bioorg. Med. Chem. Lett.* **2010**, *20*, 1724.
7. Structure deposited in the RCSB Protein Data Bank under PDB ID: 3LPB.
8. Detailed description of the biochemical assays: Gerspacher, M.; Furet, P.; Vangrevelinghe, E.; Pissot-Soldermann, C.; Gaul, C.; Holzer, P. *PCT Int. Appl. WO 2008148867*, 2008; *Chem Abstr.* **2008**, *150*, 56197.
9. Human megakaryoblastic SET-2 cells (number ACC608), DSMZ, Braunschweig, Germany) were cultured in standard RPMI medium supplemented with 10% of fetal calf serum (FCS), 2 mM L-glutamine and 1% (v/v) penicillin/streptomycin. To determine the anti-proliferative activity of candidate JAK2 inhibitors, SET-2 cells were incubated for 72 h with an 8 point concentration range of compound and cell proliferation relative to DMSO vehicle control treated cells was measured using the colorimetric WST-1 (catalog number 1644807, Roche Diagnostics GmbH, Penzberg, Germany) cell viability readout. Of each triplicate treatment the mean was calculated and these data were plotted in XLfit 4 (XLfit 4 curve fitting software for Microsoft Excel, ID business Solutions Ltd, Guildford, Surrey, United Kingdom) to determine the respective GI_{50} values.
10. Boggon, T. J.; Li, Y.; Manley, P. W.; Eck, M. J. *Blood* **2005**, *106*, 996.
11. Faller, B.; Ertl, P. *Adv. Drug Delivery Rev.* **2007**, *59*, 533.
12. Box, K. J.; Cromer, J. E. A. *Curr. Drug Metab.* **2008**, *9*, 869.
13. Pharmacokinetic properties were determined in conscious, fed, permanently cannulated female rats. For po administration by gavage, aq solutions of compounds **24–26** in PEG200 (50%) were used as a vehicle (2.5 mL/kg), whereas for the iv route compounds **24–26** were administered into the femoral vein as a solution in NMP (30%) in PEG 200 (0.5 mL/kg). Blood samples (approx. 70 μ L) were collected from the femoral artery 48 h after iv administration and for 24 h after oral dosing. Iv and po administration was in the same animals with a 48 h washout period between administrations (cross-over design). After CH_3CN precipitation of blood samples (50 μ L), dried residues were re-dissolved in methanol/water, separated by HPLC on a C18 reversed-phase HPLC column, followed by MS/MS analysis on a triple quadrupole mass analyzer (Finnigan TSQ Quantum). The compound was detected as a fragment of its protonated quasi-molecular ion $[M+H]^+$. A structurally closely related compound was used as analytical standard. Quantification of blood levels of the parent compound was based on a seven-level calibration curve (in triplicate) using blank rat blood samples spiked with stock solutions of external and internal standards. Pharmacokinetic parameters were estimated using a non compartmental approach. AUCs iv and po were calculated using the trapezoidal rule, then extrapolated to infinity using the terminal half-life calculated by log-linear regression from the last three (measurable) blood levels after iv administration.